Two-dimensional collective pinning and vortex-lattice melting in a-$Nb_{1-x}Ge_x$ films

P. Berghuis and P. H. Kes
Kamerlingh Onnes Laboratory, Leiden University, P.O. Box 9506, 2300 RA Leiden, The Netherlands
(Received 8 June 1992)

Current-voltage (I-V) and ac-resistivity measurements in the mixed state of amorphous $Nb_{1-x}Ge_x$ ($x \approx 0.3$) films in perpendicular magnetic fields are extensively analyzed for evidence of different vortex-lattice (VL) phases. In the low-temperature-field (T-B) regime flux flow is suppressed due to the presence of weak pinning centers giving rise to collective pinning of straight vortices. Various criteria for the depinning current are discussed and the impact on the collective pinning analysis is investigated. In the high T-B regime, just below the mean-field transition line $B_{c2}(T)$, linear I-V behavior shows evidence of uniform flux flow. The flux-flow resistivity follows the theoretical predictions providing a means to determine the upper critical field. It turns out to be distinctly larger than the field B_0 at which the pinning disappears or the field B_p where the pinning force starts to decrease sharply. In the narrow regime between B_p and B_0 the ac resistivity ρ_{ac} rises steeply towards the dc flux-flow resistivity. Either B_p or B_0 coincides with the VL melting field $B_m(T)$ as was predicted by the theory for two-dimensional melting. Two scenarios are further investigated: one in which B_p is taken to be B_m, so that the steep rise in ρ_{ac} is caused by inhomogeneous flow of the viscous vortex liquid in presence of disorder. In the other B_0 is identified with B_m and the behavior of ρ_{ac} is supposed to be evidence of thermally activated hopping of VL defects. The latter scenario is in better agreement with the experiments.

I. INTRODUCTION

It has been assumed that in conventional, low-T_c type-II superconductors the pinning energy U is much larger than the thermal energy kT and that therefore, thermally activated creep of flux bundles under influence of a driving force[1] only occurs close to the critical current density J_c. Recent experiments on thin films and state of the art superconducting wires suggest that far more significant thermal effects can occur, namely that thermal fluctuations can cause melting of the vortex lattice (VL). An experimental indication for VL melting was found by Hebard and Fiory[2] in very thin Al films at very low external fields. An indication of VL melting at higher fields, i.e., closer to the mean-field transition line $H_{c2}(T)$ has recently been reported by Gammel, Hebard, and Bishop[3] for thin films of the amorphous composite In/InO_x. Evidence for a universal resistive behavior of thermally activated origin in two-dimensional (2D) superconducting amorphous $Mo_{1-x}Ge_x$ films has been given by Graybeal and Beasley.[4] For multifilamentary Nb_3Sn and Nb-Ti wires a large temperature-field regime in which the magnetization is reversible, has been observed by Suenaga *et al.*[5] The line between reversible and irreversible (pinning) behavior follows quite nicely the predictions for a three-dimensional (3D) melting line.[6] In a brief account of this paper,[7] we showed that in thick amorphous films a 2D vortex lattice, i.e., a VL in which the vortices can be considered to be straight,[8] shows a melting transition below $H_{c2}(T)$. Finally, many accounts for a VL phase transition have been given for the high-temperature superconducting cuprates.[9]

In our investigations of thermal effects in low-T_c superconductors we studied the I-V response and ac resistivity of amorphous $Nb_{1-x}Ge_x$ films ($x \approx 0.3$) with thicknesses ranging from $d = 92.5$ nm to $d = 2.35$ μm in magnetic fields perpendicular to the film surface. The advantages of this system are threefold:

(1) For thin enough films (typically $d < 5$ μm) it has been shown[8,10,11] that $L_c > d/2$, where L_c is the longitudinal ($\|H$) correlation length of the VL. In such films the behavior of the critical current density J_c versus flux density B is well described by the theory of two-dimensional collective pinning (2DCP),[12] which provides essential information about the pinning strength and the VL disorder. Dealing essentially with a lattice of straight vortices, one might expect that 2D melting of the VL could be observed upon approach of $B_{c2}(=\mu_0 H_{c2})$.

(2) Critical current values in these films are roughly three orders of magnitude smaller than in the high-temperature superconductors (in a-$Nb_{1-x}Ge_x$ J_c is of order 10^5 A/m^2), while the thermal energy kT is typically only one order of magnitude smaller. Hence, assuming $U \propto J_c$ the ratio U/kT might be small enough to observe creep effects.

(3) The a-NbGe films are weak-coupling superconductors in the extreme dirty limit.[13] Therefore the dirty-limit expressions as derived by Gor'kov[14] can be supposed to hold reasonably well. Various characteristic superconducting parameters can then be derived from the experimentally obtained quantities T_c, $S = -dB_{c2}/dT|T_c$, and ρ_0, the normal-state resistivity at $T = 0$.

Our experiments show that at relatively low fields and temperatures, flux pinning dominates at small currents. Far above the critical current, uniform flux flow occurs.

A comparison with flux-flow theory in Sec. III provides an independent criterion for the mean-field transition line $H_{c2}(T)$. Around this line the conductivity is governed by fluctuation effects, which can be well described by an interpolation formula for thick films. In Sec. IV, we concentrate the discussion on the definition of the critical current and the consequences of this criterion and the values of B_{c2} for the flux-pinning analysis in terms of 2DCP theory. In Sec. V the interesting behavior at high temperatures and fields is investigated. The combined critical current and I-V data demonstrate irrevocably that the VL undergoes a phase transition in accord with the Berezinskii-Kosterlitz-Thouless theory for 2D melting.[15–17] The behavior in the narrow field interval at the crossover from a pinned VL to a uniformly moving vortex liquid is compared to predictions of dislocation mediated vortex creep (plastic creep[18]) and visco-elastic flow of the 2D flux liquid just above the melting transition.[19,20]

II. SAMPLE PREPARATION AND CHARACTERISTICS

Four amorphous $Nb_{1-x}Ge_x$ films ($x \approx 0.3$) of different thicknesses (see Table I), were prepared by either rf sputtering (I and III) or rf magnetron sputtering (II and IV). The samples were deposited on water-cooled sapphire windows (the sample with $d = 92.5$ nm was cooled with liquid N_2). The amorphousness was confirmed by x-ray diffraction and the average stoichiometry was determined by electron microprobe analysis (samples I, III, and IV) and Rutherford backscattering (sample II). On a microscopic scale the differences in the preparation method can affect the stoichiometry and the defect structure of the films, which then influence the pinning and superconducting properties.

Using photolithography, a four-probe geometry was made, in order to perform the resistivity and I-V measurements. Typically, the width was 1 mm and the voltage-probe separation 5 mm. Table I gives the thickness, Ge concentration and various superconducting parameters of the films. As has been mentioned above, these parameters can be determined from ρ_0, T_c, and S. The values for $B_{c2}(0)$ follow from the analysis of the resistivity and I-V data as given in Sec. III B. The normal-state resistivity ρ_n, was measured down from room temperature. It almost depends linearly on T with a small temperature coefficient $\rho_n^{-1} d\rho_n/dT \approx -10^{-4}$ K^{-1}. The critical temperature T_c was determined from the midpoint of the resistive transition in zero applied field. The transition widths are less than 20 mK, indicating the good homogeneity of the samples.

The I-V measurements were performed at a constant T in various perpendicular fields. In addition, ac resistivity ρ_{ac} was measured using a lock-in technique at a frequency of 721.2 Hz with a noise level of less than 1 nV. Small ac currents were applied in order to maintain a linear I-V response, typically $I \lesssim 10$ μA, which corresponds to $J \lesssim 10^5$ A/m^2 for $d = 0.1$ μm.

III. I-V RESPONSE IN THE MIXED STATE

A. Typical behavior

From the characteristics of the I-V curves three different B-T regimes can be distinguished, see Fig. 1 of Ref. 7: (1) A low-field pinning regime (1) with a non-detectable voltage below a finite critical current I_c ($\gtrsim 10$ μA), and a linear I-V response for currents far above I_c. The dynamic resistance $R_d = dV/dI$ reveals uniform flux flow. (2) A narrow, intermediate field regime (2) in which the I-V behavior is linear both at small and large currents. The ac technique only probes the linear low-current response. $R_d(I=0)$ quickly rises with increasing field, while $R_d(I \gg I_c)$ essentially follows the flux-flow prediction. (3) A high-field flux-flow regime (3) with zero critical current and ohmic I-V characteristics in the entire current-voltage range. It is our purpose to discuss the physics behind the various current-voltage behaviors.

B. Determination of H_{c2}

At sufficiently large currents the differential resistivity saturates to a constant value $\rho_{d,L}$. The field dependence of $\rho_{d,L}$ was determined at the same average flux-line velocity $v = E/B$, namely 0.2 m/s. In the pinning regime (1) the currents at this velocity are roughly an order of magnitude larger than I_c. Typically, $\rho_{d,L}$ increases monotonously in regime (1), shows a small drop in regime (2), and increases almost linearly with field in the purely ohmic regime (3) until the normal-state resistivity is reached, see Fig. 2 of Ref. 7 and also Fig. 5(b).

We first compare the $\rho_{d,L}(B)$ data in regime (3) with the predictions for the flux-flow resistivity ρ_f in dirty superconductors just below B_{c2}:[21,22]

$$\rho_f/\rho_n \approx 1-\alpha(T)(1-b) , \tag{1}$$

where $b = B/B_{c2}$. Identifying $\rho_{d,L}$ with ρ_f we obtain α and B_{c2} from a linear fit to the data. The results $\alpha(t)$ for all four samples are given in the inset of Fig. 1. It is seen that the results do not depend on thickness. Theoretically, $\alpha(t)$ depends on the inelastic-scattering time τ_i (Ref. 21) expressed in terms of a parameter $\Gamma \equiv \hbar/(2kT_c\tau_i)$.

TABLE I. Parameters of the a-$Nb_{1-x}Ge_x$ films

Sample	d [nm]	Conc. [x]	T_c [K]	ρ_0 [10^{-8} Ωm]	κ	$\lambda(0)$ [nm]	$\xi(0)$ [nm]	$B_{c2}(0)$ [T]	$B_c(0)$ [mT]
I	92.5	0.28	3.00	193	76.7	842	6.70	5.03	38.8
II	205	0.26	3.37	197	75.9	802	6.45	5.46	42.4
III	565	0.35	2.93	222	77.0	913	7.23	4.32	33.2
IV	2350	0.30	3.00	212	73.1	884	7.38	4.18	33.6

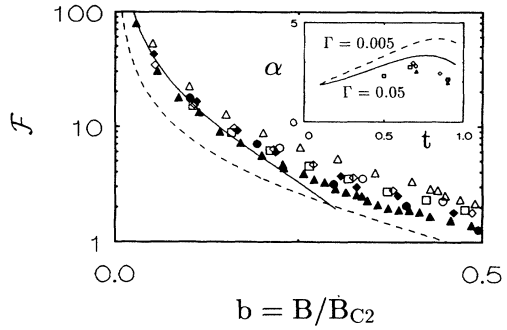

FIG. 1. The function $\mathcal{F}(b)$ of Eq. (2) for samples I (Δ, ▲), II (○,●), III (◇,◆), and IV (□) at $T\simeq 0.7$ (open symbols) and $t\simeq 0.9$ (solid symbols). The solid line displays the expected behavior for T close to T_c in the circular-cell approximation (Ref. 27). The dashed line represents the Bardeen-Stephen limit at $T=0$ (Ref. 22). The inset shows a comparison of $\alpha(t)$ with theory (Ref. 21) for sample I (△), II (○), III (◇), and IV (□). The solid and dashed lines show the theoretical $\alpha(t)$ for two values of the material parameter Γ.

The lines in the inset of Fig. 1 represent the predictions for $\Gamma=0.05$ and $\Gamma=0.005$. To get a rough estimate for τ_i, we used $\tau_i^{-1}\approx 5.2\times 10^9\ \mathrm{T^2\,s}$, obtained by Poon, Wong, and Drehman[23] for amorphous Lu compounds, thus yielding $\Gamma\approx 0.03$ at $T=2$ K. The expected temperature dependence of α is satisfactorily reproduced by our data, although the absolute values are smaller by about 20 percent. This may be due to a larger Γ value for a-Nb_3Ge. Our $\alpha(t)$ results are reminiscent to data for PbIn alloys obtained from flux-flow resistivity[24] and microwave surface resistance.[25]

An important consequence of the identification of the $\rho_{d,L}(B)$ with ρ_f is that B_{c2} can be determined from the criterion $\rho_{d,L}(B_{c2})=\rho_n$. The B_{c2} values we obtained this way, see Fig. 3 of Ref. 7, agree within 2% with the theory of Werthamer, Helfland, and Hohenberg.[26] The theoretical result can be written as $B_{c2}(T)=B_{c2}(0)f(t)$, where $B_{c2}(0)=0.69\times ST_c$. S has been determined by a least-squares fit of $f(t)$ to the $B_{c2}(t)$ data. The corresponding $B_{c2}(0)$ values are given in Table I.

In a more conventional approach B_{c2} is determined as the midpoint of a low-current resistivity transition or by the extrapolation of ρ to 0. If we use our ac resistivity measurements to determine $B_{c2}(t)$ according to these criteria, we get considerable deviations from the prediction of Ref. 26: up to ±6% for the midpoints and up to ±17% for the $\rho=0$ results.

We conclude that the good agreement of $\alpha(T)$ and $B_{c2}(T)$ with theory justifies the identification of $\rho_{d,L}$ at high fields with ρ_f. This yields a determination of B_{c2} independent of the condition F_p or $I_c\rightarrow 0$. The value of B_{c2} is an important parameter in the analysis of collective flux pinning, to be shown in Sec. IV B. It is also an important parameter for both the analysis of $\rho_{d,L}$ at low fields and the excess conductivity above B_{c2}, which is given in the following sections.

C. Low-field flux-flow resistivity

The low-field behavior of $\rho_{d,L}$ is compared to the theory for ρ_f at low fields.[12] The flux-flow resistivity for large κ materials at $b\ll 1$ in the Ginzburg-Landau regime ($t=T/T_c\lesssim 1$) can be written as

$$[\rho_f/\rho_n]^{-1}=(1-t)^{-1/2}\mathcal{F}(b)+1 \tag{2}$$

The function $\mathcal{F}(b)$ was calculated by Danilov, Kupriyanov, and Likharev[27] using a circular approximation for the hexagonal vortex cell. An interpolation formula,

$$\mathcal{F}(b)=[4.04-b^{1/4}(3.96+2.38b)]/b$$

valid up to $b\approx 0.3$, is given in Ref. 21. Only at very low fields, $b\ll 0.1$, $\mathcal{F}(b)$ reaches its limiting value $\mathcal{F}(b)=4.04/b$, which yields the Bardeen-Stephen limit[22] $\rho_f\approx b\rho_n$. The nonlinearity of $\rho_{d,L}(B)$ is clearly seen in experiment on a-Nb_3Ge films.[28] Since all parameters are known, we can directly compare our experimental $\rho_{d,L}(B)$ data with Eq. (2) by computing $\mathcal{F}(b)$. In Fig. 1 the result is given on a semilogarithmic scale for all samples at $t\approx 0.7$ and 0.9. The interpolation formula is represented by the solid line. The low-temperature prediction[22] $\rho_f/\rho_n=1.1B/B_{c2}(0)$ expressed in terms of $\mathcal{F}(B)$ is given by the dashed line. The latter deviates quantitatively from our high-temperature results, which are well described by the circular-cell approximation. As to be expected, the data at $t\simeq 0.9$ follow the theory more accurately than the $t\simeq 0.7$ data. At fields $b\gtrsim 0.2$ a clear deviation from theory appears, because the vortices start to overlap and the circular-cell approximation is not valid anymore.

D. Paraconductivity above H_{c2}

The excess conductivity $\sigma_{\mathrm{fl}}(B)$ (Ref. 29) due to superconducting fluctuations in a magnetic field above H_{c2} has been studied by various authors, both theoretically[30] and experimentally.[31] It has been shown that for dirty superconductors the direct contribution to the paraconductivity [Aslamov-Larkin (AL) term] dominates the indirect contribution (Maki-Thomson term). Since our films are dirty-limit superconductors, we compare our data with the AL term for weak-coupling superconductors in large perpendicular fields (the high-field limit). Two cases can be distinguished:[30]

(i) For thin films ($d<\xi(T)$) the excess conductivity can be written as

$$\sigma_{\mathrm{fl}}=\frac{4\pi kT}{3D}\frac{e^2}{h^2}\frac{R_B^2}{d}\ , \tag{3}$$

where D is the diffusion constant of the conduction electrons, which for the dirty limit is given by $D\simeq 8k/2\pi eS$.[9] For our films $S\approx 2.25$ T/K, which yields $D=4.9\times 10^{-5}$ $\mathrm{m^2/s}$. The length R_B is defined as

$$R_B\equiv\left[\frac{h}{2\pi eB}\ln^{-1}\left[\frac{T}{T_{c2}(B)}\right]\right]^{1/2}\ , \tag{4}$$

where $T_{c2}(B)$ is the mean-field transition temperature in a field B. Close to $T_{c2}(B)$ R_B can be written as

$$R_B \approx [\phi_0 S T_{c2}(B)/\pi B(B-B_{c2})]^{1/2} .$$

(ii) For bulk samples the paraconductivity is given by

$$\sigma_{fl} = \frac{4\pi kT}{3D}\frac{e^2}{h^2}\frac{R_B}{\sqrt{2}} . \quad (5)$$

In order to evaluate the behavior of films with $d \gtrsim \xi$, we introduce an interpolation formula between the thin-film and bulk expressions:

$$\sigma_{fl} \approx \frac{4\pi kT}{3D}\frac{e^2}{h^2}\left[\frac{R_B^2}{d}+\frac{R_B}{\sqrt{2}}\right] . \quad (6)$$

It should be noted that the relevant length scale that discriminates between thin and thick-film behavior in a field is R_B rather than ξ.

In Fig. 2 we compare our $\rho_{ac}(B)$ data above B_{c2} with the above expressions for the paraconductivity. The dotted lines display B_{c2} and ρ_n, the dashed-dotted line $\rho_f(B)$ below B_{c2}. The interpolation formula Eq. (6) is given by the solid line, the thin-film and bulk predictions Eqs. (3) and (5) by the short- and long-dashed lines, respectively. The curves were computed by substituting $D=3.3\times10^{-5}$ m^2/s, which is close to the value determined from S. It is seen that the bulk prediction does not have the correct shape. For the thin-film curve a good qualitative fit could have been obtained by adapting the value of D. However, it would then become far too small and, even worse, it would depend on temperature and film thickness. The interpolation formula also agreed well for the other temperatures and samples with a single value of D (3.3×10^{-5} m^2/s). Only at $t=0.9$ systematic deviations were seen. In this case the theoretical high-field limit may not be appropriate. Better agreement is now obtained with the low-field expression for thin films with the same D value as before. At present an interpolation formula in the low-field limit is not available.

In conclusion, the theory for thermodynamic fluctuations provides a systematic and reasonable description for the excess conductivity observed above B_{c2} in $\rho_{ac}(B)$. The role of inhomogeneities cannot be entirely ruled out, but is expected to produce a more unsystematic deviation from the normal-state conductivity. In the interpolation formula between the thin-film and bulk limit the crossover length scale R_B is both field and temperature dependent. The only adjustable parameter is found to be close to the value $D=4.9\times10^{-5}$ m^2 s^{-1} determined from the slope of H_{c2} at T_c. The fluctuation analysis depends sensitively on the $T_{c2}(B)$ curve as determined from the criterion $\rho_f(B)\to\rho_n$ for $B\to B_{c2}$. The satisfactory description of ρ_{ac} above B_{c2}, therefore, also supports this procedure for determining $B_{c2}(T)$.

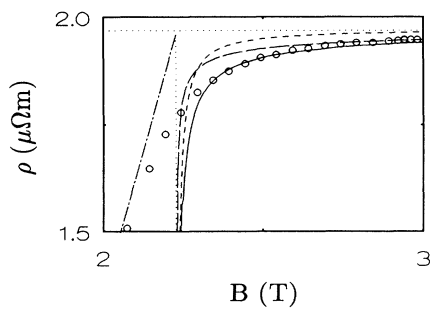

FIG. 2. Comparison of $\rho_{ac}(B)$ data (circles) of sample II at $T=2.35$ K to various models for the paraconductivity above B_{c2}. The curved lines represent $\rho_{fl}(B)$ according to Eq. (3) (short dashes), Eq. (5) (long dashes), and Eq. (6) (solid). The ρ_n and B_{c2} values are indicated by the dotted lines. The extrapolation of the $\rho_f(B)$ curve to B_{c2} is represented by the straight dashed-dotted line.

IV. COLLECTIVE PINNING

A. Determination of the critical current

The action of a driving force on the vortices ($F_d=JB$ in a J⊥B geometry), is counteracted by pinning forces arising from sample inhomogeneities. The macroscopic pinning-force density is determined from $F_p=J_cB$. Different criteria are used throughout the literature to determine J_c. We distinguish the following: (a) An arbitrary 1 μV/cm criterion is most widely adopted to determine I_c from current-voltage measurements. For our results we shall refer to these values as $I_{c,1}$. (b) I_c can also be determined from the linear extrapolation of the I-V data at high currents back to $V=0$. This critical current we define as $I_{c,L}$; the slope of the I-V data in the linear regime is $R_{d,L}$. (c) The theory of charge-density-wave (CDW) pinning suggests an additional possibility to determine I_c.[32] From the analogy between CDW and VL pinning a power-law I-V dependence is expected just above I_c, i.e., $V\propto(I-I_c)^\mu$ with $\mu\neq1$. For CDW pinning $\mu=3/2$,[32] but for 2DCP the exponent is not yet known. I_c can now be determined from the logarithmic derivative of the I-V data, i.e.,

$$\zeta\equiv[d\ln(V)/dI]^{-1}=(I-I_c)/\mu$$

for $\mu\neq0$. Note that for case (b) $\mu=1$ and thus $\zeta=(I-I_c)$.

The nature of the I-V response was investigated by plotting ζ versus I in regime (1). Typical results are shown in Fig. 3(a) for sample III at $t=0.85$. The curves are shifted horizontally for clarity. They display similar linear behavior indicative for a power-law response with the same exponent, namely $\mu=1.03\pm0.03$. Only very close to $I_{c,L}$ a different behavior sets in, see Fig. 3(b). In the low-voltage (μV) range the slope of the $\zeta(I)$ curve decreases indicating a crossover to a different power-law with a larger exponent μ, just above I_c. We estimate $\mu\approx2$ for $\zeta=0$ in agreement with the value reported for a-Zr_7Cu_3 and a-Zr_3Rh.[33] Other plausible explanations for the crossover are thermally activated motion or partial flux flow due to the distribution of pinning centers.[34]

We now evaluate definitions (a) and (b) for J_c. In Fig. 3(b), $I_{c,1}$ is indicated by the arrow. It clearly lies in the

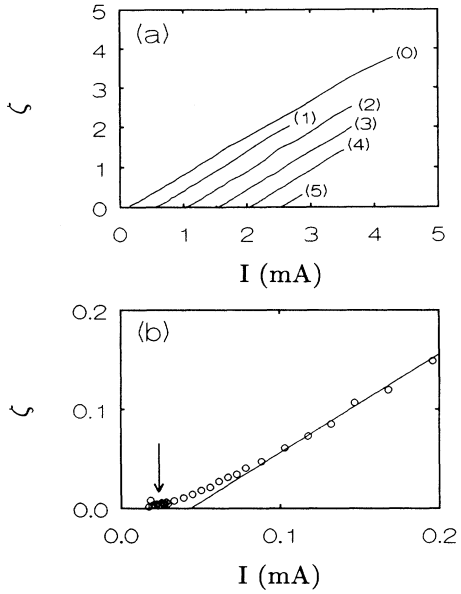

FIG. 3. The logarithmic derivative $\zeta(I)$ of the I-V data in regime (1) for sample III at $T=2.49$ K. The curves in (a) as marked by the numbers 0–5 were obtained at fields of 0.05, 0.10, 0.15, 0.20, 0.30, and 0.50 T. Each curve (n) is shifted by a horizontal offset of $n\times 0.5$ mA. In (b) the 0.5 T data (circles) are shown on an expanded scale. The line represents a linear fit, $\mu=1$, to the high current data, the arrow indicates the $I_{c,1}$ value.

nonlinear part of the I-V curves. As will be discussed in the next section, this nonlinearity affects the field dependence of $I_{c,1}$. Another way to reveal the characteristics of the I-V curves is to plot the derivative $R_d(I)=dV/dI$ versus I. These plots show a broad transition from a pinned VL with $R_d=0$ to a depinned VL with a constant level $R_{d,L}$ at large currents. It turns out that the $I_{c,L}$ values can be well identified by a single criterion, namely, $R_d=(0.75\pm0.05)R_{d,L}$. The $I_{c,1}$ values, on the other hand, correspond to $R_d\approx 0.35R_{d,L}$ at low fields, whereas $R_d\approx 0.15R_{d,L}$ fits better for fields near regime (2). Although there is no fundamental reason for either of the above criteria, the more systematic behavior of the $I_{c,L}$ data is preferable from a phenomenological point of view.

B. Collective-pinning analysis

In this section we discuss the consequences of the different critical current criteria (a) and (b) and the new definition of B_{c2} for the collective-pinning analysis. In Fig. 4(a) the macroscopic pinning force F_p computed for both criteria is plotted versus $b=B/B_{c2}$ for sample III at $T=1.99$ K ($t=0.68$). The $F_{p,L}$ values (open triangles) are about a factor of 2 larger than $F_{p,1}$ (open circles). The solid triangles represent $F_{p,L}$ data determined in the regimes (2) and (3) characterized by $R_d\neq 0$ at $I=0$. It is seen that both $F_{p,1}$ and $F_{p,L}$ vanish before B_{c2} is reached in contrast to the results of our previous analysis[8] in which the upper critical field was defined by the extrapolation of the $F_{p,1}(B)$ curves to zero. We define three specific fields: (i) The fields $b_{st,1}$ (dotted arrow) and $b_{st,L}$ where the onset of a peak in $F_{p,1}$ and $F_{p,L}$ is observed. At higher temperatures this peak disappears. The peak effect in $F_{p,1}$ has been previously observed for various weak-pinning amorphous alloys.[35] It is a rather common feature of systems with weak pinning.[36,37] (ii) The field b_p ($\simeq b_{st,L}$) indicated by the dashed arrow where the sharp downturn in $F_{p,1}$ occurs. This field corresponds to the crossover to regime (2) and the onset of the peak in $F_{p,L}$. (iii) The field b_0 where both $F_{p,1}$ and $F_{p,L}$ go to 0. It is indicated by the solid arrow and corresponds to the field at the crossover from regime (2) to (3).

In Ref. 8 it was demonstrated that pinning in various amorphous superconducting films could be well described

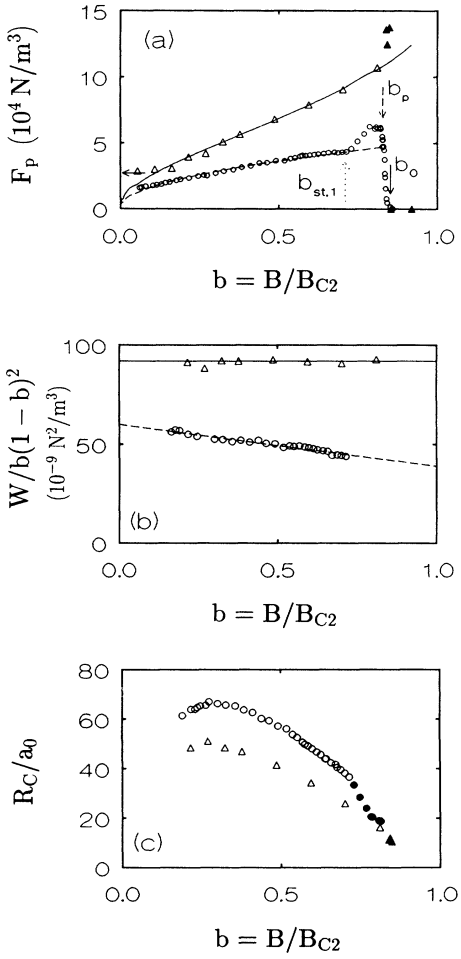

FIG. 4. Plots of (a) F_p, (b) $W/[b(1-b)^2]$, and (c) R_c/a_0 vs reduced field B/B_{c2} for sample III at $t=0.68$. The circles represent data obtained from the 1 μV criterion, the triangles data from the linear extrapolation to $V=0$. The solid triangles in (a) and (c) denote data in regime (2) where $dV/dI\neq 0$ for $I=0$. The solid circles in (c) show results in the peak regime between $b_{st,1}$ and b_p.

by the collective-pinning theory for a VL with only 2D disorder. This theory relates the pinning-force density to the pinning strength $W=n_p\langle f^2\rangle\approx\frac{1}{2}n_p f_p^2$ and the transverse correlation length R_c according to

$$W=(2r_p c_{66} dF_p)X^{1/2}(w/R_c) \tag{7}$$

and

$$R_c=(2r_p c_{66}/F_p)^{1/2}X^{1/4}(w/R_c)\ . \tag{8}$$

Here n_p is the concentration of point pinning centers with an elementary pinning force f with maximum f_p. For overlapping vortices ($b\gtrsim 0.2$) the range of the pins is $r_p\approx a_0/2$. The function $X(w/R_c)\simeq 2\pi/\ln(w/R_c)$ is usually of order 1, and w is the sample width. An expression for the shear modulus of the VL c_{66} was derived by Brandt[38]

$$c_{66}=b(1-0.29b)(1-b)^2B_c^2(t)/4\mu_0\ . \tag{9}$$

From these relations and the experimental $F_p(B)$ data $R_c(B)$ and $W(B)$ can be determined.

As previously discussed,[8] the pinning in amorphous films is most likely caused by quasidislocation loops yielding a field-temperature dependence of W according to

$$W=C_{\rm dl}(t)b(1-b)^2\ . \tag{10}$$

The prefactor is given by

$$C_{\rm dl}(t)\propto n_{\rm dl}D^4B_c^2B_{c2}\left[\frac{dB_c}{dp}\right]^2, \tag{11}$$

with $n_{\rm dl}$ the concentration of dislocation loops of diameter D. The pressure dependence of B_c in the factor (dB_c/dp) has a relatively weak temperature dependence. In Fig. 4(b) we show the results for $W/b(1-b)^2$ computed from the $F_{p,1}$ and $F_{p,L}$ data of Fig. 4(a). The plot reveals that W_1 can be represented by

$$W_1=(C_{\rm dl}+C_{12}b)b(1-b)^2$$

with $C_{\rm dl}=6.3\times10^{-8}\ \mathrm{N^2\,m^{-3}}$ and $C_{12}=-2.7\times10^{-8}\ \mathrm{N^2\,m^{-3}}$.[8] On the other hand, W_L nicely follows Eq. (10) with $C_{\rm dl}=9.2\times10^{-8}\ \mathrm{N^2\,m^{-3}}$. Combining these results with Eqs. (7) and (8) yields the dashed and solid lines in Fig. 4(a). It seems that the deviating behavior of W_1 is an artifact of the rather arbitrary 1 μV/cm criterion rather than the indication of additional pinning centers,[39,40] but more systematic investigations are needed to clarify this point. For the temperatures of our experiments, ranging from $t=0.5$ to $t=0.9$, it turns out that most of the temperature dependence of $C_{\rm dl}$ is absorbed by the factor $B_c^2B_{c2}$ of Eq. (11). A typical value of $C_{\rm dl}/(B_c^2B_{c2})$ as determined from the $F_{p,L}$ data is $2\times10^{-4}\ \mathrm{N^2\,m^{-3}\,T^{-3}}$.

In Fig. 4(c) the computed values of $R_{c,1}/a_0$ and $R_{c,L}/a_0$ are shown as a function of b. The solid symbols again represent results for the peak regimes. Below $b_{st,1}$, the two critical current criteria essentially lead to the same results. It should be noted that the pinning in our materials is so weak that R_c/a_0 can attain values as large as 50. If one would be able to observe such a VL, the disorder would be very difficult to detect. The influence of the correct B_{c2} value becomes evident in a higher value of $R_{c,1}/a_0$ at $b_{st,1}$ than observed before.[35] It was shown that the onset of the peak effect is related to the creation of VL defects (edge dislocations), when the elastic limit in the VL is locally exceeded. In terms of R_c/a_0 this happened at values of order 15 to 20. The new B_{c2} determination changes this observation in the case one uses a 1 μV criterion to a value about twice as large.

As is seen in Fig. 4(a) the 1 μV-peak is not reflected in the $F_{p,L}(B)$ data. Apparently, the VL defects disappear (anneal out) when the VL moves with sufficient velocity. This phenomenon is in accord with previous observations,[8,35] but has not yet been studied in detail. It is interesting that the onset of the peak in $F_{p,L}$ now coincides with the value $R_{c,L}/a_0\simeq 15$ in agreement with the onset criterion we derived previously. That the $F_{p,1}$ data sharply decrease simultaneously with a steep increase in $F_{p,L}$ manifests the ambiguity of the 1 μV/cm criterion for the critical current. Being in regime (2), vortex flow sets in as soon as a current is applied. Nevertheless, we see a peak in $F_{p,L}$, which means that the disorder of the VL is larger and of different nature than the disorder considered in the collective-pinning theory. This strongly suggests the involvement of edge dislocations. Their role will be further discussed in Sec. V.

V. VORTEX-LATTICE MELTING

The relevant features of the experimental data in the regimes (2) and (3) can be summarized in two figures. In Fig. 5 we show the field dependence of $F_{p,1}$, $F_{p,L}$, $\rho_{d,L}$, and $\rho_{\rm ac}$ above $b=0.4$ for sample III at $T=2.49$ K. In Fig. 6 the influence of the film thickness on the resistive behavior in field at one temperature ($t\approx0.68$) is displayed.

Figure 5 shows that at b_p several features simultaneously appear: $F_{p,1}$ starts to decrease abruptly, while $F_{p,L}$ increases, $\rho_{\rm ac}$ can be first detected and grows exponentially, and $\rho_{d,L}$ starts to deviate down from the ρ_f curve that was smoothly drawn through the other $\rho_{d,L}$ data. It should be noted as well, see Fig. 1 of Ref. 7, that above b_p the I-V curves display a behavior reminiscent of thermally assisted flux flow (TAFF).[41] The essential feature of TAFF is that $R_d(I=0)\neq0$, although it may be exponentially small. True superconductivity with $R_d(I=0)=0$ is predicted for the 3D vortex glass and the 2D vortex glass at $T=0$.[42] At b_0 both $F_{p,L}$ and $F_{p,1}$ become zero, and the $\rho_{d,L}$ and $\rho_{\rm ac}$ data merge. It is also seen that the linear extrapolation of the exponentially increasing $\rho_{\rm ac}$ data intercepts the ρ_f curve at a field B^*/B_{c2} that differs slightly from b_0. In most of the regions between b_0 and $b=1$ the $\rho_{d,L}$ and $\rho_{\rm ac}$ data fall on top of the ρ_f curve indicating purely ohmic behavior and uniform flux flow without any remanent effect of pinning.

Figure 6 shows that the above characteristics for the resistivity are observed for all samples ranging in thickness from $d=92.5$ nm to 2.35 μm. It is clear that the widths of the ohmic regimes increase with decreasing thickness. At higher temperatures the width is even larger, e.g., in the 92.5 nm film at $t=0.9$ the coincidence

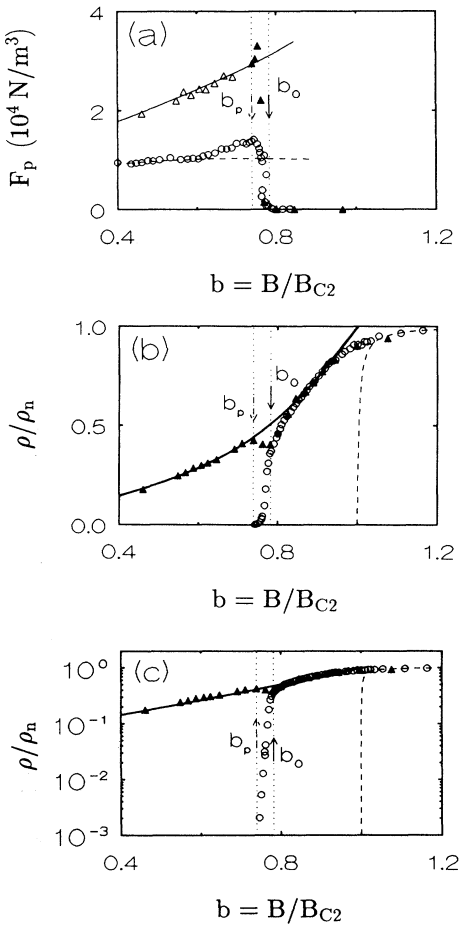

FIG. 5. Comparison between the ρ and F_p data for sample III at $T=2.49$ K. In (a) $F_{p,L}$ (△ and ▲ in case $dV/dI\neq 0$ at $I=0$) and $F_{p,1}$ data (○) are given together with the expectations of the 2DCP theory (solid and dashed lines). In (b) and (c) $\rho_{d,L}$ (▲) and ρ_{ac} data (○) are given together with the estimated $\rho_f(b)$ curve (solid line) and the $\rho_{fl}(b)$ curve computed according to Eq. (6) with $D=3.3\times10^{-5}$ m^2/s. At b_0, F_p goes to 0, at b_p, $F_{p,1}$ starts to decrease abruptly.

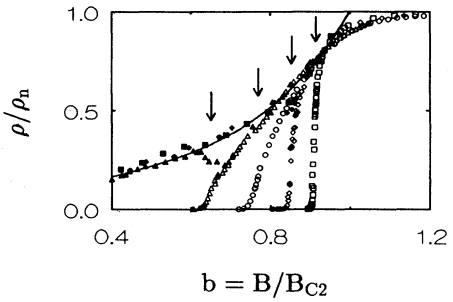

FIG. 6. Resistivity vs b for the four a-$Nb_{1-x}Ge_x$ samples at about the same reduced temperature $t\approx0.68$. The open symbols represent the $\rho_{ac}(b)$ data for sample I at $T=2.1$ K (△), II at 2.35 K (○), III at 1.99 K (◇), and IV at 1.98 K (□). The solid symbols represent the $\rho_{d,L}(b)$ data at the same temperatures and the solid line displays the estimated $\rho_f(b)$ curve. The arrows indicate the respective b^* values.

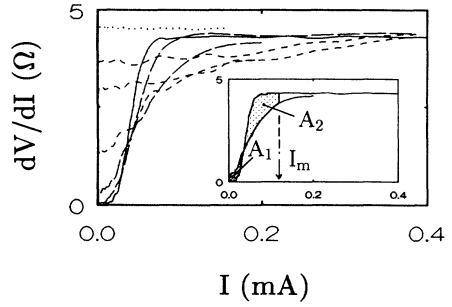

FIG. 7. $R_d(I)$ curves in the crossover regime between pinning and purely ohmic behavior for sample III at $t=0.85$. The lines represent the results for $B=0.673$ (solid), 0.680, 0.687 (long dashes), 0.694, 0.702, 0.712 (short dashes), and 0.729 T (dots). The inset shows the definition of the areas A_i for $i=1,2$.

of $\rho_{d,L}$ and ρ_{ac} occurs at $b\simeq0.6$ and $\rho_{ac}\rightarrow0$ at $b=0.35$. The broadening of the flux-flow regime is in agreement with the inverse proportionality of the vortex liquid regime with film thickness, i.e., $(B_{c2}-B_m)\propto d^{-1/2}$, with $B_m(T)$ the 2D-melting field.

Before discussing the evidence for VL melting, we like to point out that a useful way of presenting the downturn of $\rho_{d,L}$ between b_p and b_0 is a plot of dV/dI $(=R_d)$ versus I for various fields, as given in Fig. 7 for the same sample. The dotted curve, measured at $B_0=0.729$ T, represents the regime where R_d is constant in the entire current range. The solid curve is measured at B_p and displays the behavior when pinning occurs. The dashed $R_d(I)$ curves show both a nonzero R_d at $I=0$ and a distinct broadening of the transition to saturation. It follows that the downturn is in part an artifact of the criterion we used to determine $\rho_{d,L}$, namely $v=0.2$ m/s, corresponding to a current of about 0.2 mA. At much higher currents, where R_d has saturated, no minimum in $\rho_{d,L}$ would have been observed. Similar minima in the resistivity have been measured in various materials, e.g., in weak-pinning Nb alloys[35,43] and recently, in thin amorphous MoGe films by Iye *et al.*[44] In these resistance measurements V_m is recorded at constant I_m during a field or temperature sweep. In the inset of Fig. 7 it is illustrated how such a resistance minimum is related to the shape of the $R_d(I)$ curves. V_m will decrease when $A_1<A_2$.

A. Evidence for a melting transition

The system under investigation here consists of a disordered lattice of straight vortices. The implications of the Kosterlitz-Thouless (KT) theory for 2D melting[15,16] in such a system with weak disorder have been discussed in Refs. 17 and 45, and more recently by Tešanović[46] and Fisher, Fisher, and Huse.[47] At the transition the VL becomes unstable to the unbinding of thermally created dislocation pairs. The bulk shear modulus c_{66} drops sharply to zero when the vortex-lattice melting criterion is fulfilled:

$$A\frac{c_{66}a_0^2 d}{kT}\equiv A\frac{U_m}{kT}=4\pi\ . \tag{12}$$

The renormalization of c_{66} due to nonlinear lattice vibrations and VL defects are absorbed in the parameter A, which ranges between 0.4 and 0.7.[17] Both Hebard and Fiory[2] and Gammel, Hebard, and Bishop[3] found $A\sim 0.5$. Substituting Eq. (9) for c_{66} one finds that the melting line $B_m(T)$ follows from

$$B_m(T)=B_{c2}(T)\left[1-\left[\frac{16\pi\mu_0 B_{c2}(T)kT}{(1-0.29b_m)AB_c^2(T)\Phi_0 d)}\right]^{1/2}\right]. \tag{13}$$

An important question is whether the VL is depinned by thermal fluctuations before the melting line is reached from below. The criterion for thermal depinning turns out to be very similar to Eq. (12). Extending the work of Vinokur, Kes, and Koshelev[18] to the large field situation of overlapping vortices one readily finds that thermal depinning would occur when $\langle u^2\rangle_T\approx r_p^2\approx a_0^2/4$. The mean-square displacement of the vortices is given by

$$\langle u^2\rangle_T=\frac{kT}{4\pi c_{66}d}\ln(R_c^2/a_0^2)\ . \tag{14}$$

If Eqs. (14) and (12) are compared for the conditions at b_p (where $R_c\simeq 15a_0$) it is immediately seen that $B_p(T)$ lies *below* the depinning line and the same holds for $B_0(T)$. Thus, in case of weak pinning, 2D melting takes place prior to thermal depinning.

In Ref. 7 we found that the $B_0(T)$ data for all our samples coincided well with the prediction of Eq. (13) with $A\simeq 0.5$. A more sensitive way of comparing theory and experiment is provided by Fig. 8, where

$$(c_{66}a_0^2 d/4\pi kT)^{-1}\equiv(U_m/4\pi kT)^{-1}$$

is plotted versus T/T_c. According to Eq. (12) the melting line should manifest itself as a horizontal line at $(U_m/4\pi kT)^{-1}=A$. Although the scatter is appreciable, it is seen from Fig. 8(b) that the data for B_0 are indeed best described by a constant $A=0.5$. In the same figure we also show the results taking B_p and B^* as the definition of the melting field. The scatter is too large for one of the criteria to be indisputably preferable, so that this question remains to be answered by more precise experiments. However, the obvious scaling with d^{-1} and the close vicinity of all results with the prediction of Eq. (12) with a reasonable value of the renormalization parameter A, is sufficient support for the conclusion that the vortex lattice melts either a at b_p, or at b^* (the latter is preferred above b_0, since it is better defined experimentally).

B. Vortex flow about the melting line

Since it could not be decided whether B_p or B^* is the field at which the VL melts, the interpretation of the flow behavior above B_p is twofold. In both cases, however, we believe that the dip in $\rho_{d,L}$, the sudden appearance of ρ_{ac}, the TAFF-like shape of the I-V curves (Fig. 1 in Ref. 7), as well as the broad transition seen for the dashed lines in Fig. 7, give evidence for partial motion of the VL determined by a high density of edge dislocations, as has been recently described by Koshelev[48] and Shi and Berlinski.[49] The two emerging interpretations we now discuss in more detail are based on this assumption and the choice of B_p or B^* for the melting field.

When B^* is identified with the melting field the sudden increase of ρ_{ac} may be seen as a precursor effect of the melting transition caused by *thermally activated motion of edge-dislocation pairs* with formation energy U_e.[18] The smallest energy is obtained for the smallest pairs, i.e., vacancies or interstitials, for which

$$U_e=A_e c_{66}a_0^2 d=A_e U_c(t)(1-b)^2$$

with A_e a constant order unity and $U_c=\pi\xi^2 d(B_c^2/2\mu_0)$. For a-NbGe films U_c is of order $1.5\times 10^4(1-t)d$ K, if d is expressed in μm. From the values of b^* it follows that $U_e/kT\approx 30$ for $\rho_{ac}\rightarrow\rho_f$.

The other relevant energy scale for this problem is the activation barrier caused by the random potential of the

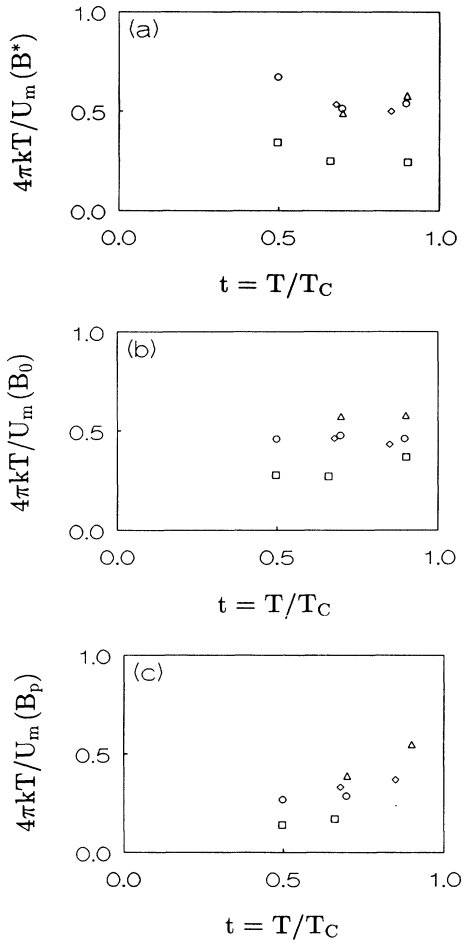

FIG. 8. Plot of $(U_m/4\pi kT)^{-1}$ vs t at three different fields: (a) B^*, (b) B_0, and (c) B_p as defined in the text. Data for various samples denoted as in Fig. 6.

pinning centers. The variance of the pinning energy over a distance a_0 is estimated as $\sigma \approx (Wa_0^2 d)^{1/2} r_p$. This supposedly provides a good estimate for the activation barrier of a VL interstitial or vacancy. The energy σ can be of the same order of magnitude as the thermal energy kT. If we assume pinning by quasidislocation loops and substitute approximate values for $B_c(0) \approx 40$ mT,

$$C_{\rm dl}/B_c^2 B_{c2} \approx 2\times 10^{-4}\ {\rm N^2\,m^{-3}}\ ,$$

$B \approx 1T$, and take $r_p = a_0/2$, we obtain

$$\sigma = 4\times 10^4 d^{1/2}(1-b)(1-t^2)\ {\rm K}$$

with d in m. For $d = 0.2$ μm, $b = 0.8$, and $t = 0.7$ this gives $\sigma \approx 2.5$ K comparable to the thermal energy. Thus, upon approach of B_m the defects can move easily due to thermal activation and the resistivity is mainly determined by the density n_d of the defects. If $U_e \gg \sigma$ the density of thermally created defects is given by[18] $n_d \approx a_0^{-2} e^{-U_e/kT}$, so that the resistivity can be written as

$$\rho \approx \rho_0 e^{-U_e/kT} e^{-\sigma/kT}\ . \tag{15}$$

It is expected that $\rho_0 \approx \rho_f$.

In Fig. 9 typical $\rho_{\rm ac}$ vs B data in the transition region ($B_p < B < B^*$) is shown for sample III at $T = 2.49$ K ($t = 0.85$). The solid line represents a fit of Eq. (15) to the data using W_L in the expression for σ, $A_e = 2/\pi$, and adapting ρ_0. The best fit is obtained for $\rho_0 = 11$ Ωm. For the other samples and temperatures similar results were obtained, except for the thickest sample (IV) where $A_e = 0.31$ gave the best fit.

All ρ_0 were many orders of magnitude larger than ρ_f, in fact, ρ_0/ρ_f ranges between 1.2×10^7 and 1.5×10^9 without much systematics. The reason for this large deviation should be found in the form of the exponential factor, i.e., $(U_e+\sigma)/kT$. We have the feeling that the density of defects is much larger than given by only considering the formation energy U_e and ignoring the increase of entropy related to the creation of defects. Taking the entropy into account would lead to $\rho_0 \approx \rho_f e^{+S/k}$ in Eq. (15). From the range of ρ_0/ρ_f we estimate $S/k \approx 19$. We believe this entropy contribution cannot be ignored close to the melting transition, because the KT melting criterion itself essentially depends on it. From the size of the sample ($\sim 10^{-5}$ m^2) and the size of the defect ($\sim a_0^2 \sim 3\times 10^{-15}$ m^2) one finds about 3×10^9 different sites for each defect. This would lead to $S/k \simeq 22$, quite close to the value that follows from ρ_0/ρ_f. We conclude, therefore, that the explanation of the increase of $\rho_{\rm ac}$ in terms of hopping of thermally created VL defects is not ruled out by our experimental results.

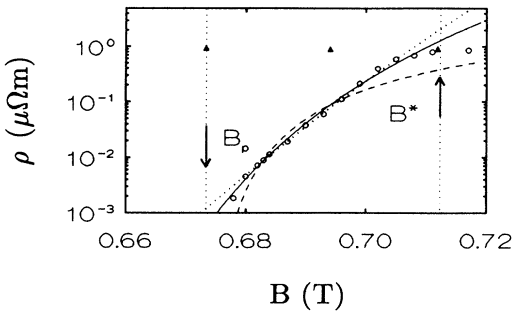

FIG. 9. $\rho_{\rm ac}(B)$ data (circles) and $\rho_{d,L}$ data (solid triangles) for sample III at $T = 2.49$ K together with the theoretical expectation according to Eqs. (15) (solid line) and (17) (dashed and dotted line). In the first case the vortex motion is seen as a precursor of melting at B^*, in the second case B_p is considered to be the melting field.

A quite different situation arises if the drop of F_p at B_p is taken as evidence for the melting transition. The increase of $\rho_{\rm ac}$ would then reveal a property of the 2D vortex liquid just above the melting point. As has been pointed out, e.g., in Refs. 17, 19, and 20, the fluid for $B > B_m$ will be very solid like out to length scales of the vortex-vortex positional correlation length, $\xi_+(B)$, which diverges extremely rapidly as $B - B_m$. Considering such a fluid as a solid with a dilute concentration of free dislocations $n_f \approx \xi_+^{-2}$, the shear viscosity is obtained as[19,20]

$$\eta \sim (n_f a_0^2)^{-1} \sim \xi_+^2(B) \sim e^{c/|B-B_m|^\nu}\ , \tag{16}$$

with $\nu = 0.3696$. The flow of the very viscous flux liquid will be affected by pinning if $\xi_+ > R_c$. The following model might then describe the situation when a driving force is applied. Some regions in the fluid may be pinned stronger than other regions. The latter start to flow under the influence of the driving force, while the former regions remain fixed by the stronger pinning. The partial flow of the flux liquid would then be dictated by the shear viscosity instead of the flux-flow viscosity. The resulting vortex mobility would, therefore, be proportional to η^{-1} and the resistivity would be given by

$$\rho = \rho_0 e^{-c/|B-B_m|^\nu}\ . \tag{17}$$

Theoretical estimates for the quantities ρ_0 and c are not available at present.

The dashed line in Fig. 9 shows a typical result of a fit of Eq. (17) with fixed values of $B_m = B_p$ and $\nu = 0.37$, varying only ρ_0 and c. Of course, ρ_0 is very sensitive to changes in c. As is seen, the dashed line starts to deviate from the data points well below B^*.

The dotted line depicts the result of a fit procedure in which B_m was allowed to lie slightly below B_p, and c was taken to be close to the average value, which was 7. We note that other ways of checking the validity of Eq. (17), e.g., by plotting $(d\ln\rho/dB)^{-1/(1+\nu)}$ versus B, produced too much scatter. The dotted line was obtained by taking $B_m = 0.64$ T, $c = 8.7$, and $\rho_0 = 2.4\times 10^5$ Ωm. The low value of B_m is hard to accept, since there are no special features observed at this field. Therefore, we prefer the first procedure with $B_m = B_p$. In this case the field regime in which data and theory can be compared is very narrow, so that a reliable check requires much more data with a higher degree of accuracy and, thus, a definitive conclusion about the positioning of the melting field cannot yet be made.

VI. SUMMARY

Our experiments on thin-film superconductors with weak pinning centers showed that the transition to a resistive state in a magnetic field has a thermally activated nature. As a consequence, the full transition to the normal state broadens, which leads to an underestimation of B_{c2} when conventional criteria like $\rho=0.5\rho_n$ or $\rho\rightarrow 0$ are used. Instead, we demonstrated that the differential resistivity $\rho_{d,L}$ in the linear regime of the I-V curves could be well identified with the flux-flow resistivity ρ_f, so that B_{c2} may be determined from the linear behavior of the $\rho_f(B)$ curves below B_{c2} by extrapolation to $\rho_f=\rho_n$. The rounding of the $\rho_f(B)$ curves about B_{c2} could be well explained by superconducting fluctuation effects. The correct value of B_{c2} agrees very well with the dirty-limit theory,[26] but is appreciably larger than before, the difference being inversely proportional to the film thickness.

The nature of the I-V curves suggested to differentiate between three field regimes. In the low-field regime flux pinning is important. The pinning properties were analyzed in terms of the 2DCP theory. It turns out that the correct value of B_{c2}, which plays an important role in this analysis, does not change the characteristic features qualitatively, especially when the critical current is defined as the current at which the linear I-V curves for $I>I_c$ extrapolates to zero. In the high-field regime the resistance is ohmic and it is essentially determined by the flux-flow viscosity. In the narrow intermediate field regime the pinning force steeply drops to zero and the flux flow is clearly nonuniform. The field at which this happens is identified as the field at which the flux-line lattice melts according to melting in 2D in presence of weak disorder (pinning). However, it could not be definitely established whether the melting field should be identified with the field at which F_p starts to decrease or that it is the field at which F_p becomes zero. In the first case the sharp increase of $\rho(I=0)$ with field might be explained by the steep increase of the shear viscosity of the vortex fluid when the melting field is approached from above. In the second case this resistivity increase is seen as a precursor for melting and is thought to be due to creep of thermally created VL defects, i.e., interstitials and vacancies. In view of the present experimental data we could, unfortunately, not decide which of these models should be preferred.

An essential ingredient of the analysis was that the dimensionality of the disorder is 2. This is a consequence of the weakness of pinning in amorphous superconducting films. The weak-pinning condition is not fulfilled in many cases. Strong pins give rise to a highly disordered VL,[12] because the vortices adapt to the underlying pin distribution. In such materials, due to the broad distribution of elementary pinning forces, flux-flow through channels of weaker pinning can occur. This nonuniform flow is evidenced by highly nonlinear I-V curves in the pinning regime.

Note added in proof. A crossover from 2D to 3D melting is expected for thicker films at d_{cr}. As pointed out to us by Koshelev an estimate of d_{cr} shows that our thickest film ($d=2.35$ μm) is well in the 3D regime with regards to melting, although the collective pinning remains 2D. This explains why the squares in Fig. 8 systematically lie below the data of the thinner films. A paper is in preparation to discuss further the details of the crossover.

ACKNOWLEDGMENTS

We acknowledge the experimental assistance of A. L. F. van der Slot and instructive conversations with D. R. Nelson, V. M. Vinokur, and A. E. Koshelev. This project was financially supported by the Foundation for Fundamental Research on Matter (Stichting FOM).

[1] Y. B. Kim, C. F. Hempstead, and A. R. Strnad, Phys. Rev. Lett. **9**, 306 (1962); P. W. Anderson, *ibid.* **9**, 309 (1962).

[2] A. Hebard and A. T. Fiory, Physica B **109&110**, 1637 (1982).

[3] P. L. Gammel, A. F. Hebard, and D. J. Bishop, Phys. Rev. Lett. **60**, 144 (1988); Phys. Rev. B **40**, 7354 (1989).

[4] J. M. Graybeal and M. R. Beasley, Phys. Rev. Lett. **56**, 173 (1986).

[5] M. Suenaga, A. K. Gosh, Youwen Xu, and D. O. Welch, Phys. Rev. Lett. **66**, 1777 (1991).

[6] D. R. Nelson, Phys. Rev. Lett. **60**, 1973 (1988); E. H. Brandt, *ibid.* **63**, 1106 (1989); A. Houghton, R. A. Pelcovits, and A. Sudbø, Phys. Rev. B **40**, 6763 (1989).

[7] P. Berghuis, A. L. F. van der Slot, and P. H. Kes, Phys. Rev. Lett. **65**, 2583 (1990); P. Berghuis, Ph.D. thesis, Leiden University, 1991.

[8] P. H. Kes and C. C. Tsuei, Phys. Rev. B **28**, 5126 (1983).

[9] D. J. Bishop, P. L. Gammel, D. A. Huse, and C. A. Murray, Science **255**, 165 (1992).

[10] A dimensional crossover from a 2D to a 3D disordered VL, accompanied with an order of magnitude increase of J_c was observed in films with $d>5$ μm, see Ref. 11.

[11] R. Wördenweber and P. H. Kes, Phys. Rev. B **34**, 494 (1986).

[12] A. I. Larkin and Yu. Ovchinnikov, J. Low Temp. Phys. **34**, 409 (1979).

[13] C.C. Tsuei, in *Superconducting Materials Science*, edited by S. Foner and B. Schwartz (Plenum, New York, 1981), p. 735.

[14] See, e.g., L. P. Gor'kov, Zh. Eksp. Teor. Fiz. **36**, 1918 (1959) [Sov. Phys. JETP **9**, 1364 (1959)]; L. P. Gor'kov, Zh. Eksp. Teor. Fiz. **37**, 1407 (1959) [Sov. Phys. JETP **10**, 998 (1960)]; M. Tinkham, *Introduction to Superconductivity* (McGraw-Hill, New York, 1980).

[15] V. L. Berezinskii, Zh. Eksp. Teor. Fiz. **61**, 1144 (1971) [Sov. Phys. JETP **34**, 610 (1972)].

[16] J. M. Kosterlitz and D. J. Thouless, in *Progress in Low Temp. Physics*, edited by D. F. Brewer (North-Holland, Amsterdam, 1978), Vol. VII-B.

[17] D. S. Fisher, Phys. Rev. B **22**, 1190 (1980), and references cited therein.

[18] V. M. Vinokur, P. H. Kes, and A. E. Koshelev, Physica C **168**, 28 (1990).

[19] D. R. Nelson, in *Phase Transitions and Critical Phenomena*, edited by C. Domb and J. L. Lebowitz (Academic, London, 1983), Vol. 7.

[20] A. Zippelius, B. I. Halperin, and D. R. Nelson, Phys. Rev. B

22, 2514 (1980).
[21]A. I. Larkin and Yu. Ovchinnikov, in *Non Equilibrium Superconductivity*, edited by P. N. Langeberg and A. I. Larkin (North-Holland, Amsterdam, 1986).
[22]J. Bardeen and M. J. Stephen, Phys. Rev. **140**, 1197 (1965); L. P. Gor'kov and N. B. Kopnin, Zh. Eksp. Teor. Fiz. **65**, 396 (1973) [Sov. Phys. JETP **38**, 195 (1974)].
[23]S. J. Poon, K. M. Wong, and A. J. Drehman, Phys. Rev. B **31**, 1668 (1985).
[24]P. Hagmann, R. Meier-Hirmer, and H. Winter, Z. Phys. B **26**, 233 (1977).
[25]R. P. Huebener, R. T. Kampwirth, and A. Seher, J. Low Temp. Phys. **2**, 113 (1970).
[26]N. R. Werthamer, E. Helfland, and P. C. Hohenberg, Phys. Rev. **147**, 295 (1966).
[27]V. V. Danilov, M. Yu. Kupriyanov, and K. K. Likharev, Fiz. Tverd. Tela **16**, 935 (1974).
[28]A. Pruijmboom, E. van der Drift, and P. H. Kes, Physica C **165**, 179 (1990).
[29]W. J. Skocpol and M. Tinkham, Rep. Prog. Phys. **38**, 1049 (1975).
[30]K. D. Usadel, Z. Phys. **227**, 260 (1969); K. Maki, J. Low Temp. Phys. **1**, 513 (1969); H. J. Mikeska and H. Schmidt, Z. Phys. **230**, 239 (1970); G. E. Clarke and D. R. Tilley, J. Phys. C **3**, 2448 (1970); K. Aoi, R. Meservey, and P. M. Tedrow, Phys. Rev. B **9**, 875 (1974).
[31]B. Serin, R. O. Smith, and T. Mizusaki, Physica **55**, 224 (1971); R. R. Hake, Physica **55**, 311 (1971).
[32]D. S. Fisher, Phys. Rev. Lett. **50**, 1486 (1983).
[33]F. de la Cruz, J. Luzuriaga, E. N. Martinez, and E. J. Osquiguil, Phys. Rev. B **36**, 6850 (1987).
[34]H. J. Jensen, A. Brass, Y. Brechet, and A. J. Berlinsky, Phys. Rev. B **38**, 9235 (1988).
[35]R. Wördenweber, P. H. Kes, and C. C. Tsuei, Phys. Rev. B **33**, 3172 (1986).
[36]R. A. French, J. Lowell, and K. Mendelssohn, Cryogenics **7**, 83 (1967).
[37]G. A. Spierings, E. Revolinsky, and D. J. Beerntsen, J. Phys. Chem. Solid **27**, 535 (1966).
[38]E. H. Brandt, Phys. Status Solidi B **77**, 551 (1976).
[39]R. Wördenweber, A. Pruijmboom, and P. H. Kes, J. Low Temp. Phys. **70**, 253 (1988).
[40]R. Wördenweber, Ph.D. thesis, Leiden University, 1986, p. 47–63.
[41]P. H. Kes, J. Aarts, J. van den Berg, C. J. van der Beek, and J. A. Mydosh, Supercond. Sci. Technol. **1**, 242 (1989).
[42]M. P. A. Fisher, Phys. Rev. Lett. **62**, 1415 (1989).
[43]H. van Beelen, Ph.D. thesis, University of Leiden, 1967.
[44]Y. Iye, A. Watanabe, S. Nakamura, T. Tamegai, T. Terashima, K. Yamamoto, and Y. Bando, Physica C **167**, 278 (1990).
[45]B. A. Huberman and S. Doniach, Phys. Rev. Lett. **43**, 950 (1979).
[46]Z. Tešanović and L. Xing, Phys. Rev. Lett. **67**, 2729 (1991).
[47]D. S. Fisher, M. P. A. Fisher, and D. A. Huse, Phys. Rev. B **43**, 130 (1991).
[48]A. E. Koshelev, Phys. Rev. B **45**, 12 936 (1992).
[49]A.-C. Shi and A. J. Berlinski, Phys. Rev. Lett. **67**, 1926 (1991).